

Analysis of the plastic wave propagation in high
velocity tension of a bar of finite length
(I. rigid-linearly work hardening material)

By

Kozo KAWATA, Shinji FUKUI and Jiro SEINO

Summary. The mechanical behaviours of a bar of finite length in high velocity tension are analyzed using characteristics basing upon strain rate independent theory, assuming rigid-linearly work hardening material property. In this case, the solution on the relation of breaking strain ϵ_b versus tensile velocity V_1 can be obtained for the all range of V_1 , though it does not exist for the values of V_1 smaller than critical impact velocity V_{cr} , in the case of a bar of semi-infinite length. The critical impact velocity exists in this case also and coincides with the value derived Kármán in the case of semi-infinite length. Strain rate effect in material properties can be determined by the difference between the theoretical results above mentioned basing upon the strain rate independent theory and experimental ones.

1. INTRODUCTION

In the field of space technology, many problems, such as hypervelocity impact by meteoroids, or high energy rate forming of vehicles, etc., are related with high velocity deformation of materials. In studying the mechanical behaviours in high velocity deformation, one of the most popular fundamental tests is high velocity tension test of a uniform bar or plate [1] [2] [3]. When we intend to investigate the variation of mechanical properties, especially breaking elongation, in high velocity deformation, it is found that theoretical result on the relation of breaking strain ϵ_b versus tensile velocity V_1 to be compared with experimental ones is not yet derived [4]. On a bar of semi-infinite length, the behaviour of plastic wave propagation had been analyzed by Kármán [5], Taylor [6], and Rakhmatulin [7], and the existence of critical impact velocity V_{cr} is shown, but the relation of ϵ_b versus V_1 is unable to be described in the range $0 < V_1 < V_{cr}$, as shown in Fig. 1. As actual tensile specimens are always of finite length, the relation of ϵ_b versus V_1 should be derived for tensile specimens of finite length.

To clarify the behaviours of tensile specimens of finite length, the plastic wave propagation is analyzed by a graphical representation using characteristics [8], assuming rigid-linearly work hardening material property. The assumption of the simple material property enables analytical derivation of some important behaviours, such as the relation of ϵ_b versus V_1 , in this case, and it is enabled to suppose the strain rate effect in high velocity elongation, basing upon the difference

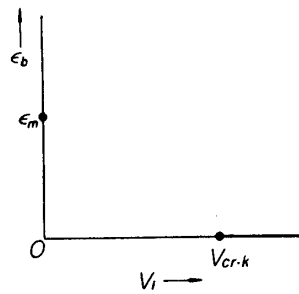


FIG. 1 The theoretical relation derived by Kármán, of breaking strain ϵ_b versus tensile velocity V_1 for a bar of semi-infinite length. ϵ_m is static breaking strain of material, and $V_{cr.k}$ is critical impact velocity.

between the theoretical results by the strain rate independent theory and experimental ones.

2. GRAPHICAL REPRESENTATION OF PLASTIC WAVE PROPAGATION BY MEANS OF CHARACTERISTICS

The equation of motion for an element initially of length dx , of a bar under tension, is

$$A\rho dx \frac{\partial^2 u}{\partial t^2} = A \frac{\partial \sigma}{\partial x} dx \quad (1)$$

$$\frac{\partial \sigma}{\partial x} = \frac{d\sigma}{d\epsilon} \cdot \frac{\partial \epsilon}{\partial x} = \frac{d\sigma}{d\epsilon} \cdot \frac{\partial^2 u}{\partial x^2} \quad (2)$$

where,

- x : Lagrange type coordinate along initially unstrained bar
- u : displacement of a section
- σ : nominal stress, force per unit initial cross-sectional area
- ϵ : strain, $=\partial u/\partial x$
- A : initial cross-sectional area of bar
- t : time
- ρ : density of material unstrained.

From (1) and (2),

$$c^2 \frac{\partial^2 u}{\partial x^2} - \frac{\partial^2 u}{\partial t^2} = 0 \quad (3)$$

where,

$$c^2 = \frac{1}{\rho} \frac{d\sigma}{d\epsilon} \quad (4)$$

The propagation of stress waves is considered for an elasto-plastic material having

the linear stress-strain relation in the plastic range as shown in Fig. 2. In this

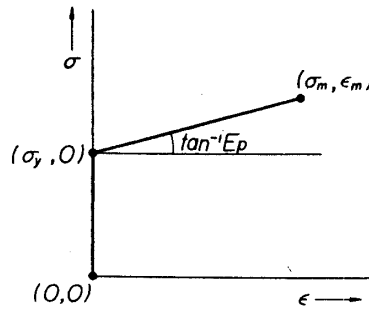


FIG. 2 Rigid-linearly work hardening material property. σ_y is yield stress. It is assumed breaking occurs instantaneously when stress reaches to σ_m .

stress-strain relation, elastic strains are neglected. That is, the material property is rigid-linearly work hardening one, as shown in (5).

$$\left. \begin{aligned} 0 \leq \sigma \leq \sigma_y \quad \epsilon = 0 \\ \sigma_y \leq \sigma \quad \epsilon = (\sigma - \sigma_y) / E_p \end{aligned} \right\} \quad (5)$$

The relation is assumed to hold in high velocity deformation also. In the elastic range, c is the velocity of elastic wave propagation and a constant $c_0 = \infty$. In the plastic range, c is the velocity of plastic wave propagation and a constant, as follows:

$$c^2 = E_p / \rho \quad (6)$$

In this case, general solution of (3) is given by

$$u = f(x + ct) + F(x - ct) \quad (7)$$

where f and F are arbitrary functions. The characteristic lines in (x, t) -plane for (3) are, [8]

$$dx/dt = \pm c \quad (8)$$

When waves of stress discontinuity occur, the following relations are determined by the equations of continuity and momentum change,

$$(\rho cv + \sigma)_1 = (\rho cv + \sigma)_2 \quad (9)$$

for waves traveling in the positive direction, and

$$(\rho cv - \sigma)_1 = (\rho cv - \sigma)_2 \quad (10)$$

for waves traveling in the negative direction, where points 1 and 2 are just ahead and just behind of a stress wave, and c is the absolute value of the velocity of wave propagation, though stress σ and particle velocity $v = du/dt$ may take positive or negative values. Application of equations (9) and (10) enables to determine stress and particle velocity distributions in the (x, t) -plane.

3. ANALYSIS OF THE PLASTIC WAVE PROPAGATION IN HIGH VELOCITY TENSION OF A BAR OF FINITE LENGTH

We consider a bar extending from $x=0$ to $x=l$ and assume that the free end point at $x=0$ is put into motion instantaneously at $t=0$ with the constant velocity $v_1 = -V_1$ whereas the other end $x=l$ is fixed as shown in Fig. 3. When V_1 is large

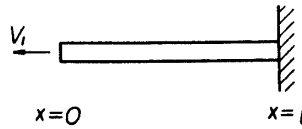


FIG. 3 High velocity tension of a bar of length l .

enough, for $t > 0$ an elastic wave front runs along the bar with the velocity $c_0 = \infty$ and the stress amplitude σ_y (yield stress of the material), and a plastic wave front follows along the bar with the velocity $c = (E_p/\rho)^{1/2}$ and the stress amplitude $\sigma_1 (> \sigma_y)$. When the elastic wave reaches the fixed end, it is reflected at the end and infinitely near elements are stressed to the stress:

$$\sigma_y \left(1 + \frac{c}{c_0} \right) = \sigma_y \tag{11}$$

The particle velocity induced by the elastic wave is

$$\int_0^{\sigma_y} d\sigma / \rho c_0 = 0 \tag{12}$$

So that, the assumption of neglecting elastic strains implies that the stress is σ_y and the particle velocity is zero in the region 0 shown in Fig. 4. The linear stress-

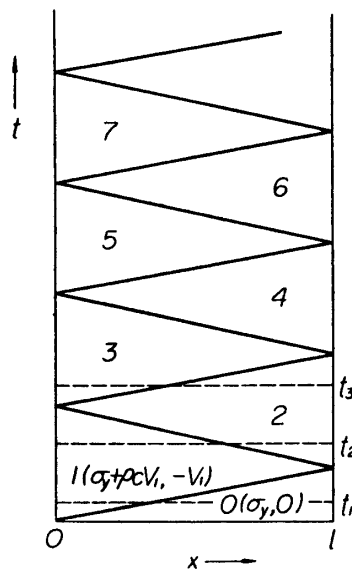


FIG. 4 Lagrange (x, t) diagram for finite bar shown in Fig. 3.

strain relation in the plastic range gives a constant wave velocity and a single plastic wave front of stress discontinuity. In the graphical representation of this case in the (x, t) -plane, we obtain a family of wave fronts showing the process of successive reflections as shown in Fig. 4. The inclinations of these fronts are,

$$dt/dx = \pm 1/c \tag{8'}$$

If the stress and the particle velocity are put equal to σ_1 and v_1 respectively, in the region 1,

$$\begin{aligned} \sigma_1 + \rho c v_1 &= \sigma_y + 0 \\ \therefore \sigma_1 &= \sigma_y - \rho c v_1 = \sigma_y + \rho c V_1 \end{aligned}$$

So that, (σ, v) in the region 1 are given as

$$(\sigma_y + \rho c V_1, -V_1) \tag{13}$$

And then,

$$(\sigma_y + 2\rho c V_1, 0) \tag{14}$$

for the region 2, and

$$(\sigma_y + 3\rho c V_1, -V_1) \tag{15}$$

for the region 3, are derived successively. Generally, (σ, v) are determined as

$$\{\sigma_y + n\rho c V_1, -V_1(1 + (-1)^{n+1})/2\} \tag{16}$$

for the region n .

The stress distributions at various times after the impact are shown in Fig. 5. The times t_1, t_2, t_3 are shown in Fig. 4. The variations of stress and strain with

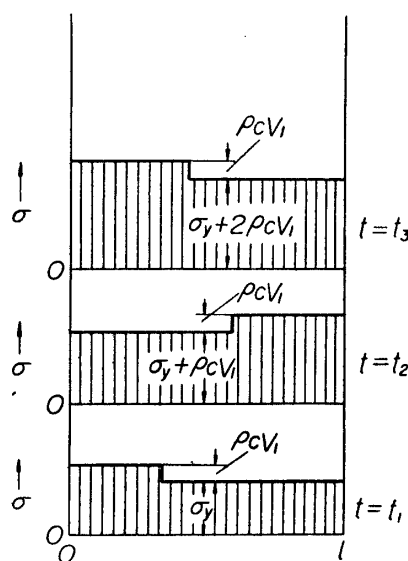


FIG. 5 Some examples of stress distribution at various times after the impact.

time at various points of the bar are shown in Figs. 6 and 7.

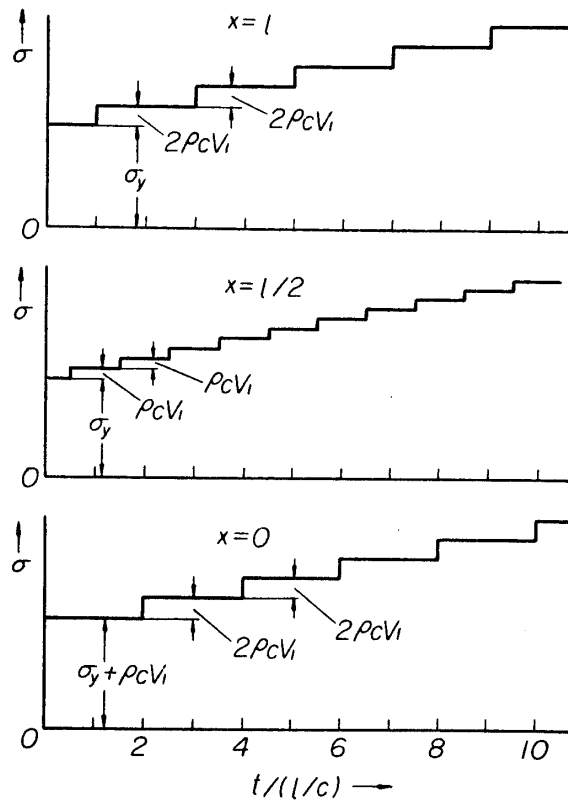


FIG. 6 The variations of stress with time at various points of the bar.

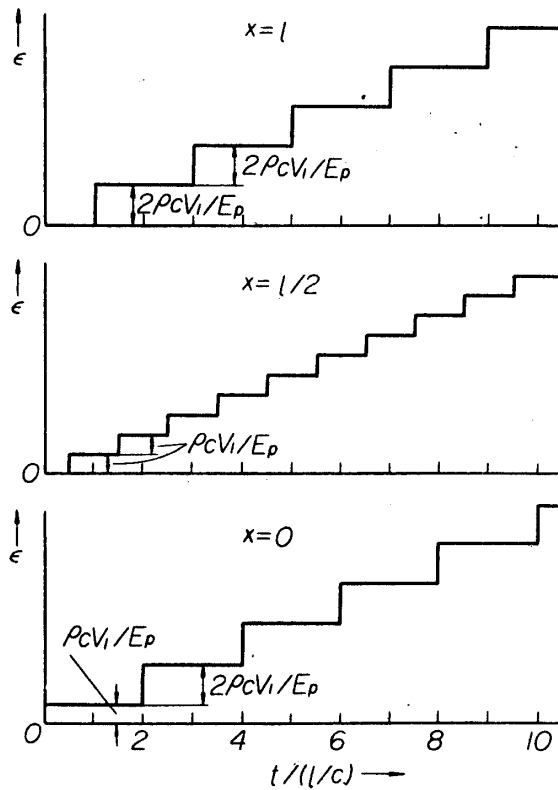


FIG. 7 The variations of strain with time at various points of the bar.

Next, the relation of breaking strain ε_b versus tensile velocity V_1 may be derived using (13)~(16). If we assume the breaking will occur instantaneously, where the condition :

$$\sigma_y + n\rho c V_1 \geq \sigma_m \quad (17)$$

are satisfied for the first time, the strain distribution at the instant of breaking is the one for which the strain corresponding to the stress: $\sigma_y + (n-1)\rho c V_1$ is uniformly distributed. So the breaking strain is

$$\varepsilon_b = (n-1)\rho c V_1 / E_p \quad (18)$$

The relation of ε_b versus V_1 is obtained as follows:

(A) a bar of semi-infinite length :

$$V_1 = (\sigma_1 - \sigma_y) / \rho c \quad (19)$$

If we assume breaking occurs when σ_1 reaches to σ_m

$$V_{cr.k} = (\sigma_m - \sigma_y) / \rho c = c \cdot \varepsilon_m \quad (20)$$

where, $V_{cr.k}$ is the critical impact velocity. This value agrees with that calculated by the formula derived by Kármán for semi-infinite bar [5]

$$V_{cr.k} = \int_0^{\varepsilon_m} c d\varepsilon \quad (21)$$

where, $V_{cr.k}$ is the critical impact velocity derived by Kármán for a bar of semi-infinite length.

(B) a bar of finite length :

(i) When

$$\sigma_y + \rho c V_1 \geq \sigma_m > \sigma_y \quad (22)$$

holds, breaking occurs at $t=0$, and $x=0$, and

$$\varepsilon_b = 0 \quad (23)$$

The condition (22) can be written in the form,

$$V_1 \geq \frac{1}{\rho c} (\sigma_m - \sigma_y) = V_{cr.k} > 0 \quad (24)$$

(ii) When

$$\sigma_y + 2\rho c V_1 \geq \sigma_m > \sigma_y + \rho c V_1 \quad (25)$$

holds, breaking occurs at $t=l/c$, and $x=l$, and

$$\varepsilon_b = \rho c V_1 / E_p = (V_1 / V_{cr.k}) \varepsilon_m \quad (26)$$

The condition (25) can be written in the form,

$$V_{cr.k} > V_1 \geq \frac{1}{2} V_{cr.k} \quad (27)$$

(n) When

$$\sigma_y + n\rho c V_1 \geq \sigma_m > \sigma_y + (n-1)\rho c V_1 \quad (28)$$

holds, breaking occurs at $t=(n-1)l/c$, and $x=l$ if n is even, or $x=0$ if n is odd, and

$$\varepsilon_b = (n-1)\rho c V_1 / E_p = (n-1)(V_1 / V_{cr.k})\varepsilon_m \quad (29)$$

The condition (28) can be written in the form,

$$\frac{1}{n-1} V_{cr.k} > V_1 \geq \frac{1}{n} V_{cr.k} \quad (30)$$

From these calculations, the plot of the relation of ε_b versus V_1 is obtained as shown in Fig. 8. The breaking strain ε_b of a bar of finite length in high velocity

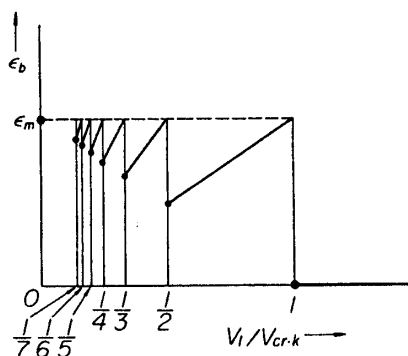


FIG. 8 The relation of breaking strain ε_b versus tensile velocity V_1 of finite bar.

tension is not always equal to the static breaking strain ε_m , but varies as shown in the figure for tensile velocity V_1 .

4. CONCLUSIONS

(1) The mechanical behaviours of a bar of finite length in high velocity tension are derived in analytical forms, by the strain rate independent theory, assuming rigid-linearly work hardening material property.

(2) In the case of a bar of finite length, the solution on the relation of breaking strain ε_b versus tensile velocity V_1 can be obtained in the form as shown in Fig. 8, for the all range of V_1 , though the solution does not exist for the values of V_1 smaller than critical impact velocity, in the case of a bar of semi-infinite length. Critical impact velocity V_{cr} exists in this case also, and coincides with the value $V_{cr.k}$ obtained by Kármán for a bar of semi-infinite length.

(3) The upper limit of dynamical breaking strain ε_b is breaking strain of material ε_m .

(4) Apparent scattering of experimental data of the relation of ε_b versus V_1 seems to depend, partially at least, upon the characteristics of the relation as shown in Fig. 8.

- (5) The relation of ϵ_b versus V_1 does not depend upon the length of the bar l .
(6) Strain rate is stepwise, and conventional strain rate V_1/l shows the mean value approximately.
(7) Because the above mentioned calculations are made by the strain-rate independent theory, strain-rate effect is added to the theoretical results, for real materials.

The strain-rate effect in material properties appears as the difference between the theoretical results such as the relation of ϵ_b versus V_1 and experimental ones.

- (8) When finite elastic strains are considered in the stress-strain relation of material, the behaviours on breaking differ from the results above mentioned. The results assuming another material properties will be reported in near future.

*Department of Materials,
Aeronautical Research Institute,
University of Tokyo, Tokyo.
March 12, 1964.*

REFERENCES

- [1] For example,
P. G. Shewmon, V. F. Zackay: *Response of Metals to High Velocity Deformation* (1961). Interscience.
M. Manjoine, A. Nadai: *Proc. ASTM*, **40** (1940), 822.
P. E. Duwez, D. S. Clark: *Trans. ASTM*, **47** (1947), 502.
D. S. Clark, D. S. Wood: *Trans. ASM*, **42** (1950), 45.
D. S. Clark: *Trans. ASM*, **46** (1954), 34.
[2] T. Tsumura, S. Sakui, K. Okamoto, T. Nakamura, et al: *Proc. Third Japan Congr. On Testing Materials* (1960), 95.
[3] S. Fukui, K. Kawata, J. Seino: *Bull. Aero. Res. Inst., Univ. of Tokyo*, **3**, No. 6A (1963), 361 (in Japanese).
[4] K. Kawata, S. Fukui, J. Seino: *Preprint, Fourteenth Japan Meeting on Plastic Working* (1963), 131 (in Japanese).
[5] Th. von Kármán, P. E. Duwez: *J. Appl. Phys.*, **21** (1950), 987.
[6] G. I. Taylor: *J. Inst. Civil Engrs (London)*, **26** (1946), 486.
[7] H. A. Rakhmatulin; *Priklad. Math. Mekh.*, **11** (1947), 379.
[8] Th. von Kármán, H. F. Bohnenblust, D. H. Hyers: *NDRC Report A-103 (OSRD 946)*, 1942.